Detection Limit of ultra-scaled Nanowire Biosensors

A. Afzalian, N. Couniot, and D. Flandre
Information and Communication Technologies, Electronics and Applied Mathematics (ICTEAM) Institute
Université catholique de Louvain (UCL)
Louvain-la-Neuve, Belgium
Aryan.afzalian@uclouvain.be

Abstract—**The fundamental detection limit of ultra-scaled Si nanowire FET (NWT) biosensors is studied with a NEGF quantum microscopic approach. For negatively charged analytes, a N-doped NWT is found to be more sensitive and to get less sensitivity degradation when increasing channel length. Our results predict threshold voltage shifts due to a single charge analyte on the order of tens to hundreds of mV in dry (air) or low ionic solution environments, which hint at single charge/analyte detection. However, the sensitivity to a single charge analyte rapidly drops down to the mV range in typical ionic solution and SAM conditions.**

Keywords: Nanowire FET, label-free biosensing, nanoscale, silicon, NEGF quantum simulation modeling.

I. INTRODUCTION

Si nanowire transistors (NWTs) are very promising as transducers and in particular for the label-free sensing and detection of biological species [1,2]. Nanowires indeed provide a very high sensitivity (S) to many analytes of interest, allowing one to sense biological phenomena with an unprecedented level of precision. There are however little simulation tools and models allowing for the understanding, prediction and co-design of such bio-electronic systems [3]. Macroscopic models and experiments have predicted S improvement when scaling down the dimension of the NWTs [1-3]. In this work, we have used our dedicated microscopic quantum simulation platform, NANOcore [4,5] to investigate the sensitivity of Si nanowire biosensors (NWTBs) scaled close to the technological limit, i.e. when S is expected to be at its optimum and quantum effects are strong.

II. SIMULATION METHODS AND STRUCTURES

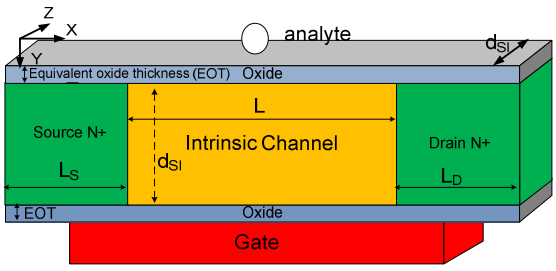

Figure 1. Schematic of the [100] SOI square cross-section N-type nanowire with floating top and lateral gates (the lateral gates are not shown) and a single analyte on the top gate.

This work was supported by the Fonds de la Recherche Scientifique (F.R.S. – F.N.R.S), Belgium and by the EU FP7 NoE NANOFUNCTION.

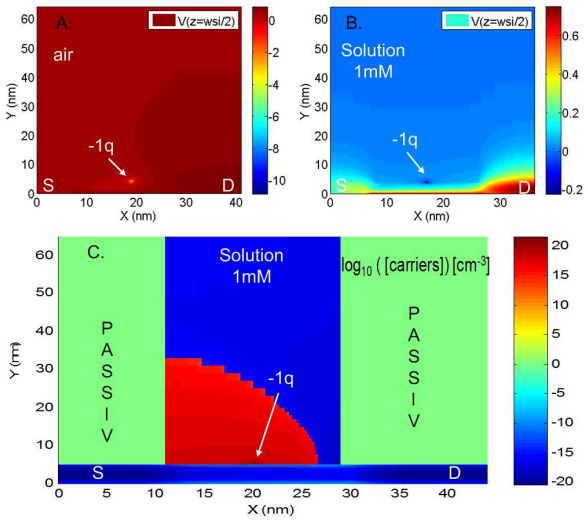

Figure 2. XY-plots in the Z-plan cutting across the middle of the NWT with a single negative charge on the top gate and a 60nm surrounding. A) Potential in air media at V_G=0.7V. B) Potential in NaCl 1mM ionic solution media at V_G=0.7V. C) Carrier concentration (electrons, ions) at V_G=-0.4V. L=20nm. S/D extensions: L_S=8nm L_D=12nm, V_D= 0.7V, doping $N^+=10^{20}cm^{-3}$. Oxide: EOT=0.5nm. t_{SAM}=0nm. T=300K.

The system under study is a square cross-section N-doped NWT of side-dimension d_{SI} with an intrinsic channel biased by a bottom gate that also serves as a reference electrode (Fig. 1). The side and top gates are left floating and consist of an oxide layer of equivalent thickness EOT on which dielectric self-assembled monolayers (SAM) can potentially be added for increasing the selectivity of the NWT. This affinity-based layer is supposed to be flat and homogenous of thickness t_{SAM} and to have a relative dielectric permittivity ε_{rSAM}. On the top gate, centered at half the length and width of the channel, an analyte of charge $z_a.q$ is placed. In this study, as we are interested to get general trends on the fundamental detection limit of ultra-scaled nanowires, we have used as analyte the smallest detectable unit, i.e. a simple electronic charge distributed in a volume of 0.25x0.25x0.25 nm^3. A surrounding media on the top and side of the NWT is considered and taken wide enough (typically from 10 to 100 nanometers) so that the results do not change when further increasing its thickness. We have considered both air and NaCl solution with an ionic

ISBN 978-0-615-71756-2

concentration c_{ion0}. Each ion species i with charge valence z_i in the solution is assumed to follow a modified Boltzmann distribution (MBD), which is essentially a Boltzmann distribution modified to include steric effects that become important at large voltage ($\Phi(r)$) through an effective ion diameter d_i [6]:

$$c_{ion,i}(r) = z_i.c_{ion0,i}\frac{e^{\frac{z_i\Phi(r)}{2U_t}}}{1+2\nu_i\sinh^2(\frac{z_i\Phi(r)}{2U_t})} \quad with \quad \nu_i = 2d_i^3.c_{ion0,i} \tag{1}$$

In (1), U_t is the thermal voltage, while ν_i is the adimensional packing parameter related to d_i (d_{Na}=3.68Å, d_{Cl}=2.42Å) [7]. For the electronic part, we have used a previously developed Self-Consistent NEGF code to simulate the nanowires [4,5]. The electronic wave functions are calculated in the Si and surrounding oxides. A (Fast-) coupled mode space ((F)CMS) is chosen as it is much faster than a real space approach, while conserving the required accuracy by preserving the mode coupling in the vicinity of the perturbation potential of the charged analytes [4]. The Hamiltonian is written in the effective mass formalism using NWT diameter-dependent effective masses that are extracted from a $sp^3d^5s^*$ Tight-Binding Hamiltonian [4]. Phonon scattering is accounted for within the Born Self-Consistent framework [5]. The influence of the analyte and possible ions is directly included in a non-perturbative way through the electrostatic potential that is solved for in the full domain, NWT and surrounding media.

III. Simulation Results and Discussion

Simulated NWT Sensitivity to a positively S_+ or negatively S_- charged analyte for various device parameters with EOT= 0.5 nm. The sensitivity is expressed as the V_{TH} shift extracted at $I_{D,0Q}=10^{-7}$ A/µm.

d_{SI} (nm)	L (nm)	S_- (mV/q)	S_+ (mV/q)	t_{SAM} (nm) (ε_{SAM} =2.3)	media
2	20	-145	58	0	air
3	20	-97	68	0	air
4	20	-61	56	0	air
6	20	-84	86	0	air
3	60	-69	11	0	air
3	100	-16	3	0	air
2	20	-32	29	0	water c_{ion0}=0
2	20	-20	10	0	water c_{ion0}=1mM
2	20	-1	1	0	water c_{ion0}=100mM
2	20	-3	3	2.5	water c_{ion0}=1mM
2	20	-1	1	5	water c_{ion0}=1mM
3	20	-65	62	2.5	air

We first investigate the impact of the cross-section on the sensitivity of 20nm long N-NWTs in the air (Fig. 3A and Table 1). When in presence of a positively (+q case) or negatively (-q case) charged analyte, the $I_D(V_G)$ characteristics are shifted in opposite directions (Fig. 5). The sensitivity is estimated here in mV/|q|, both for a positive (z_a=1) and negative (z_a=-1) charge, i.e. respectively S_+ and S_-, as the shift in threshold voltage, ΔV_{th}, when compared to the uncharged case (z_a=0, 0q case) (see Table 1). ΔV_{th} is the gate voltage shift in the characteristics needed to achieve same current in both charged and uncharged cases at a given reference current, $I_{D,0q}$ or equivalently $V_{G,0q}$ (Id or V_G of the uncharged case). Notice also that although staying on the same order of magnitude, ΔV_{th} has a tendency to decrease when increasing the inversion level of the NWTs, i.e. ΔV_{th} is a slightly decreasing function of I_D or V_G (Fig. 4A). This is because the slope of the $I_D(V_G)$ characteristics is slightly modified by the presence of the charged analyte (inset of Fig. 4B). For the –q case the slope is improved as the negative charge pushes the channel closer to the back gate, therefore improving gate coupling, while in the +q case, the positive charge attracts the electron channel closer to the front gate, therefore degrading back gate coupling. In any cases, the sensitivity to a single charge is as high as several tens to hundreds of mV, translating in order of magnitudes changes in current levels in subthreshold regime (Fig. 4).

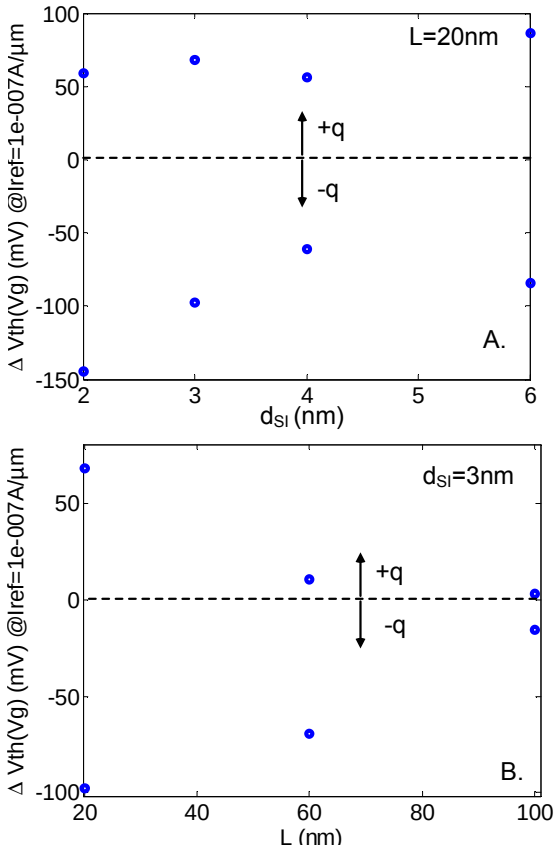

Figure 3. Simulated NWT V_{TH} shift compared to the 0q case for a charged analyte with z_a=-1 and +1, extracted at $I_{D,0q}=10^{-7}$ A/µm in air A) in function of d_{SI} with L=20nm, B)) in function of L with d_{SI} =3nm. V_D=0.7V. EOT= 0.5nm. t_{SAM}=0nm.

The general trend, however, is the reduction of NWT sensitivity when increasing d_{SI} as could be expected. An exception is to be noted for S_+ of the d_{SI}=2nm NWT and for d_{SI} =6nm, as will be explain below. Also a dissymmetry can be observed: $|S_-|$ is larger than S_+. This dissymmetry is strongly enhanced when the channel length is increased up to 60 and 100nm as S_+ reduces much faster when increasing L than S_- (Table 1, Fig. 3B and Fig. 5). This can be understood as a negative charge repeals electrons and therefore locally creates

a barrier in the conduction band that shifts the top of the channel barrier (TCB) and therefore V_{th} upward, while a positive charge locally lowers the electron energy and results in a potential well that shift TCB and V_{th} downward (Fig. 6). The smaller the cross-section, the higher the barrier or the deeper the well.

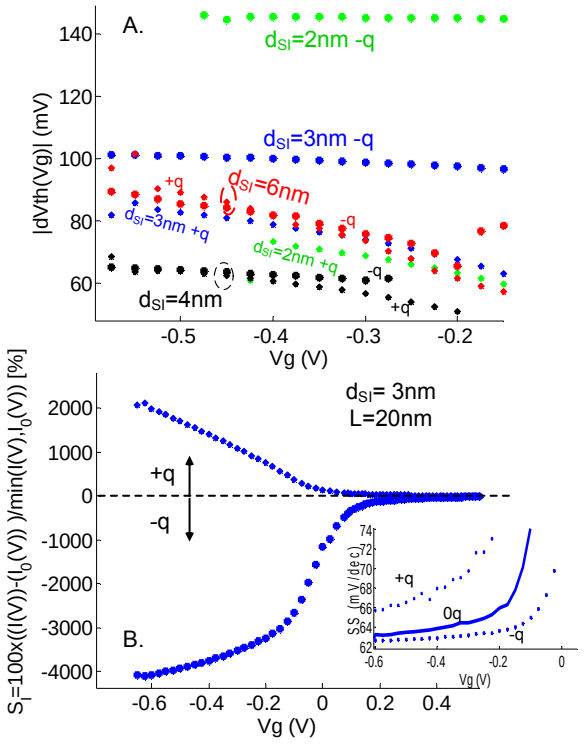

Figure 4. A) Absolute value of the V_{TH} shift for a charged analyte with z_a=-1 and +1 in function of V_G of the 0q case in air for different d_{SI}. ΔV_{th} has a tendency to decrease when increasing the inversion level or the NWT, i.e. ΔV_{th} is a slightly decreasing function of I_D or V_G. This is because the slope of the $I_D(V_G)$ characteristics is slightly modified compared to the 0q case by the presence of a charged analyte as shown in the inset of Fig. 4.B for the d_{SI}=3nm case . B) Related relative current variation (%) in function of V_G for the d_{SI}=3nm case. The threshold voltage shift due to a single charge is as high as several tens to hundreds of mV, translating in order of magnitudes changes in current levels in subthreshold regime. L=20nm. V_D=0.7V. EOT= 0.5nm. t_{SAM}=0nm.

In the barrier case, because TCB is located at the barrier itself, the sensitivity is directly linked to the barrier height generated by the charge. Furthermore, the (slow) decrease of sensitivity with L is due to the stronger inelastic scattering in the longer channel that allows for more electrons with an initial energy lower than the barrier to acquire the required energy to cross it (Fig. 6A and 6D). On the other hand, the V_{th} shift and therefore S_+, is not linked directly to the depth of the potential well, but to its efficiency to lower TCB, hence a reduced sensitivity compare to the barrier case. Furthermore, this efficiency to lower TCB rapidly decreases in intensity as L is increased (Fig. 6C and 6F). Also despite a deeper well, for the L=20nm case, a smaller S_+ is observed for d_{SI}=2nm than d_{SI}=3nm. This is linked to a coupled effect between the positive charge and a stronger drain voltage influence for d_{SI}=3nm that further lowers the right-side of the energy subband and increases source – drain (SD)-tunneling (Fig. 6C). This effect, which is enhanced by short channel effects that increase with d_{SI}, explains why for the L=20nm cases no clear reduction of S_+ is observed for the increasing d_{SI} values shown here (Fig. 3A and Table 1).

A reversal of the trends is observed for the d_{SI}=6nm value, where both S_+ and S_- are higher than the d_{SI}=4nm ones. This is linked to the fact that for d_{SI}=6nm, the confinement being weaker, the dark space region is smaller. This allows for having an electron channel that can extend and be moved closer to the oxide interfaces. This firstly compensates for the reduction of the charged analyte electrostatic influence that one would expect with a thicker cross-section: Both for d_{SI}=4 and 6nm, the TCB shift due to a negative charge is about 60meV. This secondly enhances the modification of the slope of the $I_D(V_G)$ characteristics due to the presence of the charged analyte. This in turn can enhance the sensitivity but also gives rise to more variation of S with V_G as can be observed in Fig. 4.A.

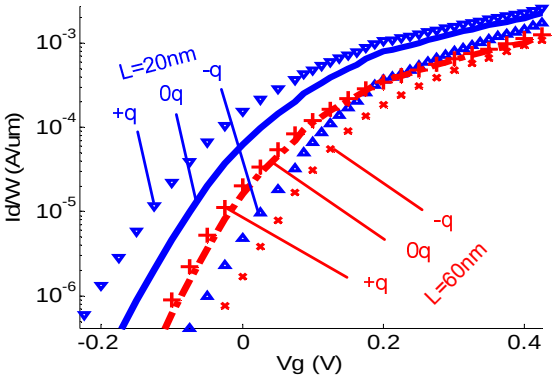

Figure 5. Simulated $I_D(V_G)$ curves of a d_{SI}=3nm NWT with L=20 and 60nm and with an analyte with z_a=-1, 0, and 1 in air. V_D=0.7V, EOT= 0.5nm. t_{SAM}=0nm.

Finally the impact of the surrounding media is investigated by comparing in Table 1 and Fig. 7A S_+ and S_- of the L=20nm 2x2 nm^2 NWT in air and in solution with c_{ion0}=0, 1mM, which is typical for buffered solutions, and 100mM, which is typical for undiluted physiological solutions. The sensitivity is strongly reduced in solution. Because of the much higher media permittivity (ε_r=80) when compared to air, the electric field related to the charge extends to a much wider region (Fig. 2), therefore creating a wider but also much smoother energy barrier perturbation. When ions are considered in the solution, the sensitivity is further reduced due to screening effect (Fig. 2C). When increasing the analyte distance from the channel by either increasing the front gate EOT or, as shown in Table 1 and Fig. 7B, introducing a SAM layer, the sensitivity is further degraded (this much more in solution than in air) as the front gate coupling is reduced.

IV. CONCLUSION

The fundamental detection limit of ultra-scaled NWTBs has been studied with a quantum microscopic approach. For negatively charged analytes, an N-doped NWT is more sensitive and gets less sensitivity degradation when increasing channel length (by reciprocity a P-doped NWT will be more sensitive to detect positively charged analytes). Our results predict S in the order of tens to hundreds of mV/q in dry (air) or low ionic solution environments, which hints at single charge/analyte detection. In this case also, the design space in terms of channel length and cross-section to get such a high sensitivity is not too severe compared to today's fabrication capabilities. However, S rapidly drops down to the mV/q range in typical ionic solution and SAM conditions. This translates in I_D variation of a few percent or less. In this case the design space to get single charge detection is quite narrow and in particular having the charge as close as possible to the surface of the sensor is crucial.

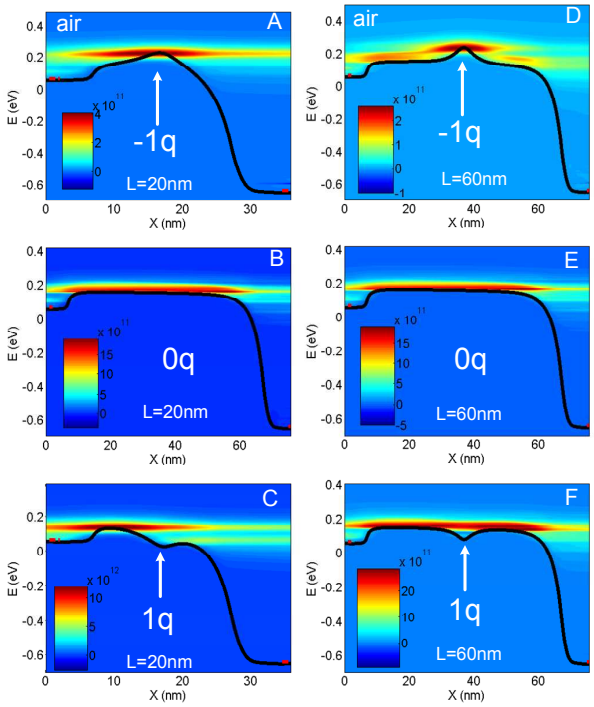

Figure 6. First Conduction subband minimum $E_{c1}(x)$ (black line) and current spectrum J(x,E) in A/J (surface plot) along the channel for the L=20nm and L=60nm d_{SI}=3nm NWTs in air with z_a=-1 (A and D), z_a=0 (B and D), and z_a=1 (C and F respectively). The position of S and D Fermi levels is also indicated by a red dot at S and D side.

REFERENCES

[1] J.-I. Hahm, C. M. Lieber, "Direct Ultrasensitive Electrical Detection of DNA and DNA Sequence Variations Using Nanowire Nanosensors", Nano Lett., vol. 4, no. 1, pp. 51−54, 2004.

[2] Stern et al., "Label-free immunodetection with CMOS-compatible semiconducting nanowires", Nature, vol. 445, no. 7127, pp. 519–522, 2007.

[3] P. R. Nair, M. A. Alam, "Design Considerations of Silicon Nanowire Biosensors", IEEE Trans. On Electon Devices, vol. 54, no. 12, pp. 3400-3408, Dec. 2007.

[4] A. Afzalian, *et al*., "A new F(ast)-CMS NEGF Algorithm for efficient 3D simulations of Switching Characteristics enhancement in constricted Tunnel Barrier Silicon Nanowire MuGFETs", Journal of Computational Electronics, Vol. 8, N° 3-4, pp. 287-306, Oct. 2009.

[5] A. Afzalian, "Computationally Efficient self-consistent Born approximation treatments of phonon scattering for Coupled-Mode Space Non-Equilibrium Green's Functions", J. of Applied Physics, Vol. 110, p. 094517, 2011.

[6] M. S. Kilic, M. Z. Bazant, and A. Ajdari, "Steric effects in the dynamics of electrolytes at large applied voltages: I. Double-layer charging", Phys. Rev. E, vol. 75, pp. 021502, 2007.

[7] P. Pham, M. Howorth, A. Planat-Chrétien, and S. Tardu, "Numerical Simulation of the Electrical Double Layer Based on the Poisson-Boltzmann Models for AC Electroosmosis Flows", COMSOL Users Conference, Grenoble, 2007.

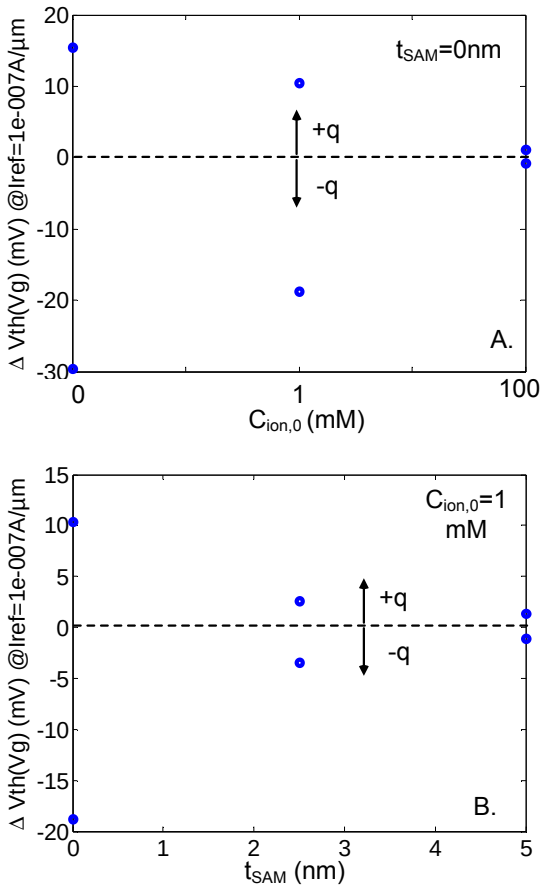

Figure 7. Simulated V_{TH} shift compared to the 0q case for a charged analyte with z_a=-1 and +1, extracted at $I_{D,0q}=10^{-7}$ A/µm in solution A) in function of c_{ion0} with t_{SAM}=0nm , B) in function of t_{SAM} with c_{ion0} =1mM. d_{SI} =2nm, V_D=0.7V. EOT=0.5nm. ε_{rSAM}=2.3.